Oxidation of Metals, Vol. 11, No. 2, 1977

The Effect of ΔT (Oxidizing Temperature Minus Cooling Temperature) on Oxide Spallation

Daniel L. Deadmore* and Carl E. Lowell*

Received December 29, 1976

Several alloys (one iron base and five nickel base) were cyclically oxidized in a series of tests in which the higher temperature (1100 or 1200°C) of the cycle was fixed at a level to allow ample oxidation in reasonable time and the lower temperature was variable to allow cycle temperature differences (ΔT_s) of up to 1400°C. The alloys oxidized included those which formed simple oxides such as Al_2O_3 or Cr_2O_3, as well as those which formed complex scales. Cooling rates were relatively low to minimize thermal shock effects. Each cycle consisted of 1 hr at the higher temperature and $\frac{1}{2}$ hr at the lower temperature. Samples were tested up to 370 cycles. The extent of attack was determined by specific weight change which was continuously monitored. For all nickel alloys, as ΔT increased the extent of spallation increased. This effect was attributed to thermal expansion mismatches between the oxide and the nickel substrate. The FeCrAl alloy was not sensitive to ΔT and resisted spalling at ΔT levels to 1400°C. FeCrAl, and the Al_2O_3 scale which forms on it, have thermal expansion coefficients which are substantially more alike than any of the other oxide–metal combinations tested.

KEY WORDS: oxidation; cyclic; spallation; stress.

INTRODUCTION

High-temperature superalloy materials frequently are used in power systems where the environments are oxidizing and the components are subjected to thermal cycling. The cycles may be of a few hours duration, as in aircraft turbines, or may be hundreds or even thousands of hours as in the

*Lewis Research Center, Cleveland, Ohio.

case of ground power turbines. Regardless of the duration of the cycle, it is the cyclic nature of the application which often causes the primary loss of material[1] due to oxide scale spallation. This cyclic dependency is due to a sequence of events as follows:

1. When the sample is heated at a constant temperature (isothermally) in an oxidizing environment, it initially oxidizes to form a relatively protective oxide scale, e.g., Al_2O_3 (assuming suitable alloy composition), which grows approximately parabolically. Parabolic growth means that the scale thickens more slowly with time since its growth is diffusion controlled. For many if not most commercial high-temperature alloys this growth rate is sufficiently low to make metal loss by isothermal oxidation negligible in terms of the effect on creep and/or stress rupture life.
2. However, as the material cools at the end of a heat cycle, thermal stresses arise which can cause part or all of the oxide that has formed to spall.
3. At the start of the second cycle, the rate of oxide scale formation is faster than at the end of the first cycle as the oxide is now effectively thinner or locally absent as a result of oxide spallation.
4. This process is repeated every cycle and in time the metal surface composition tends to change so that it can no longer form the protective oxide. In turn other oxides form and these form at higher rates.
5. With continued cycling the rate of material loss further accelerates as new, even less protective oxides form. While it is obvious that spalling upon cooling results from thermal stresses, the origin of such stresses is in some doubt. Douglass,[2] and more recently Hancock and Hurst,[3] have reviewed oxide stresses at some length. Both assume that the thermal stress arises from differences in the thermal expansion coefficients of the metal and the oxide. However, another source of thermal stress is possible, i.e., thermal shock. This stress would arise from rapid cooling of the oxide such that the oxide cools nonuniformly, as would be the case in burner-rig testing or engine use.[4]

In order to adequately model oxide spallation, and thus develop a means to predict the extent of metal loss, the relative importance of thermal stress due to mismatch in expansion and that due to thermal shock must be established. The purpose of this paper was to determine the importance of thermal mismatch stresses on oxide spallation. This purpose was addressed by examining the influence of ΔT (the exposure temperature minus the cool-down temperature) on a variety of alloys oxidized at 1100 or 1200°C.

Several cast and wrought high-temperature alloys were selected to cover a wide range of materials and compositions. The alloys were IN-601, IN-702, B-1900 plus Hf, TD-NiCrAl, HOS-875, IN-718, and nickel aluminide-coated IN-718. All samples were oxidized at either 1100 or 1200°C, depending on the oxidation characteristics of the alloy, in 1 hr cycles for up to 370 hr. The maximum temperature was chosen to allow the

characteristic oxidation to occur in reasonably short times. The temperature to which the samples were cooled was varied. The specific weight change was then determined as a function of ΔT (the oxidizing temperature minus the cooling temperature) for each alloy. The results were evaluated in terms of thermal expansion mismatch.

MATERIALS AND PREPARATION

The compositions of the alloys investigated are shown in Table I. HOS-875 is the only iron-base alloy. On oxidation, it forms a protective alumina scale and is used primarily in furnace heating elements. TD-NiCrAl is an oxide dispersion-strengthened nickel-base alloy which also forms mainly alumina during oxidation. IN-702 and IN-601 are nickel-base wrought alloys; the former relies on alumina and the latter on chromia formation for oxidation protection. IN-718 and B-1900 + Hf are cast nickel-base alloys which have complex scale formation during oxidation. The nickel aluminide coating on IN-718 was formed by a standard pack cementation process. The resultant coating forms alumina during oxidation.

Samples were machined to approximately $2.5 \times 1.3 \times 0.2$ cm (prior to coating); the HOS-875 samples were slightly longer (~3.0 cm). Before oxidation, and after measurement, the samples were rinsed in ethyl alcohol, swabbed off, and air dried.

Table I. Alloy Analysis, wt.%

Element	HOS-875[a]	TD-NiCrAl[b]	IN-702[a]	IN-601[b]	IN-718[a]	B-1900+Hf[a]
Chromium	22.25	16.22	15.6	23.04	18.6	8.0
Aluminum	5.39	4.63	3.4	1.38	0.4	6.0
Iron	Bal.	—	0.4	13.41	18.5	<0.35
Nickel	—	Bal.	Bal.	Bal.	Bal.	Bal.
Cobalt	—	—	—	—	—	10.5
Molybdenum	—	—	—	—	3.1	6.0
Niobium	—	—	—	—	5.0	<0.10
Tantalum	—	—	—	—	—	4.25
Hafnium	—	—	—	—	—	1.60
Titanium	—	—	0.7	—	0.9	1.0
Silicon	—	—	0.2	0.48	0.30	<0.25
Manganese	—	—	0.05	0.27	0.20	<0.2
Boron	—	—	—	—	—	0.015
Carbon	—	—	0.05	0.04	0.04	0.10
Thorium	—	1.78[c]	—	—	—	—

[a] Typical analysis.
[b] Analysis for this heat.
[c] Present as ThO_2 (2.03 wt.%).

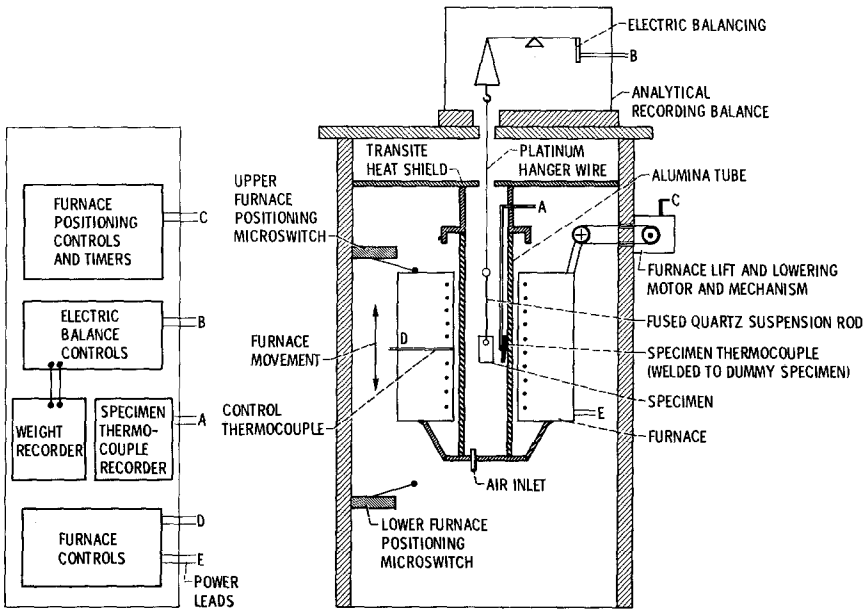

Fig. 1. Continuous weight change, cyclic oxidation apparatus for use at ambient pressure.

Cyclic oxidation was carried out in the apparatus shown in Fig. 1. The furnace can be raised or lowered by a variable speed motor between adjustable limit switches. At the start of the test the furnace is lowered and the sample suspended from the balance. A dummy sample with a thermocouple attached is positioned next to, but not touching the sample. The furnace is heated to the oxidizing temperature and the test started by raising the furnace until the sample is in the center of the hot zone. The temperature is controlled to within ±5°C. At the end of a cycle the furnace is very slowly lowered to a position determined by the lower limit switch. ΔT is a function of this position, which is maintained for the duration of the run. The samples are continuously weighed and not removed from the balance until the end of test. This technique was used for all but the maximum ΔT's—1400 and 1300°C—which were achieved by lowering the furnace to its minimum position and, after the sample had cooled to near room temperature, placing it in liquid nitrogen until all bubbling stopped. The samples were then rewarmed to room temperature in ethyl alcohol, dried, and then weighed.

A typical temperature profile is shown in Fig. 2. ΔT's were adjusted as described above. The heating and cooling times were set by individual timers. A complete list of oxidizing temperatures and ΔT's is given in Table II. $\Delta T = 0$ refers to an isothermal test.

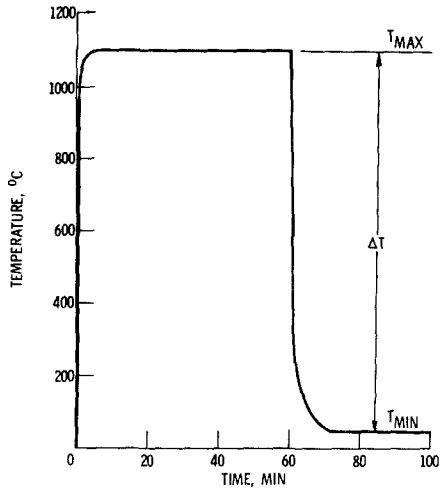

Fig. 2. Typical temperature profile for a single cycle.

At the conclusion of the tests the samples were removed and the surface oxide phases were determined by x-ray diffraction. Scanning electron microscopy was used to observe oxide surface morphology and the samples were then sectioned and examined metallographically.

RESULTS

Microscopy

Figure 3 shows the surface morphology of the oxides formed during cyclic oxidation on IN-601 and on B-1900+Hf. The microstructures in cross section are shown in Fig. 4. These structures are typical of all the alloys

Table II. Test Conditions

Alloy	T_{max}, °C	ΔT, °C
HOS-875	1200	0, 1050, 1145, 1400
TD-NiCrAl	1200	0, 1050, 1145, 1400
IN-702	1200	0, 500, 800, 1050, 1145, 1400
IN-601	1100	0, 400, 700, 950, 1045, 1300
B-1900+Hf	1100	0, 400, 700, 950, 1045, 1300
IN-718	1100	0, 560, 780, 870, 930, 1030
IN-718 coated	1100	0, 780, 1030

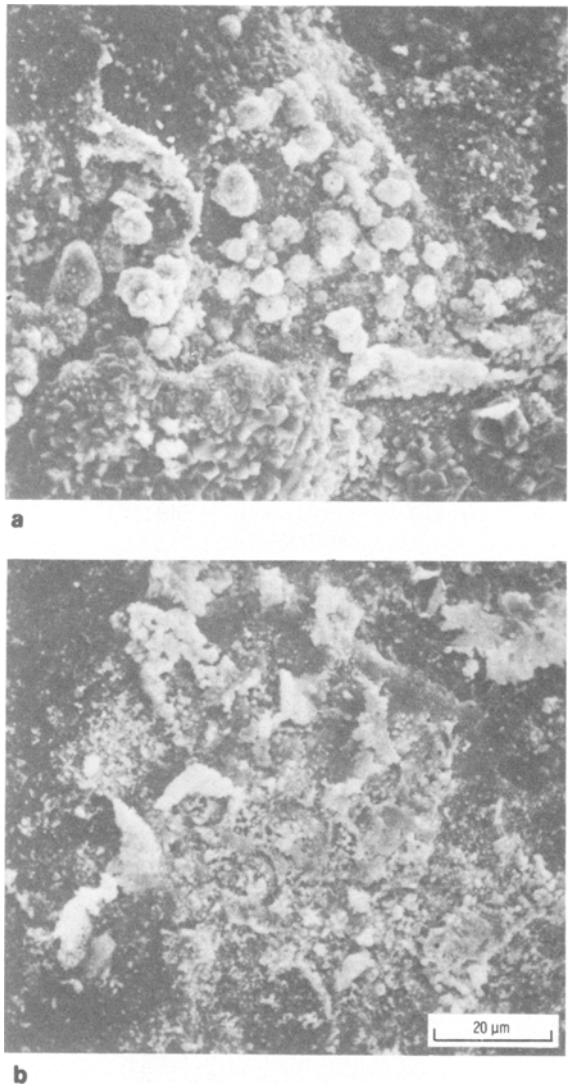

Fig. 3. Surface morphology of IN-601 (a) and B-1900+Hf (b) after 195 cycles with $\Delta T = 1300°C$.

which spalled and show that while spalling results in an irregular surface, the oxide remains as a continuous layer. No spalling to bare metal was observed on any of the samples except for the TD-NiCrAl run with $\Delta T = 0$ after it was cooled to room temperature. Except for that isolated case, oxide failure

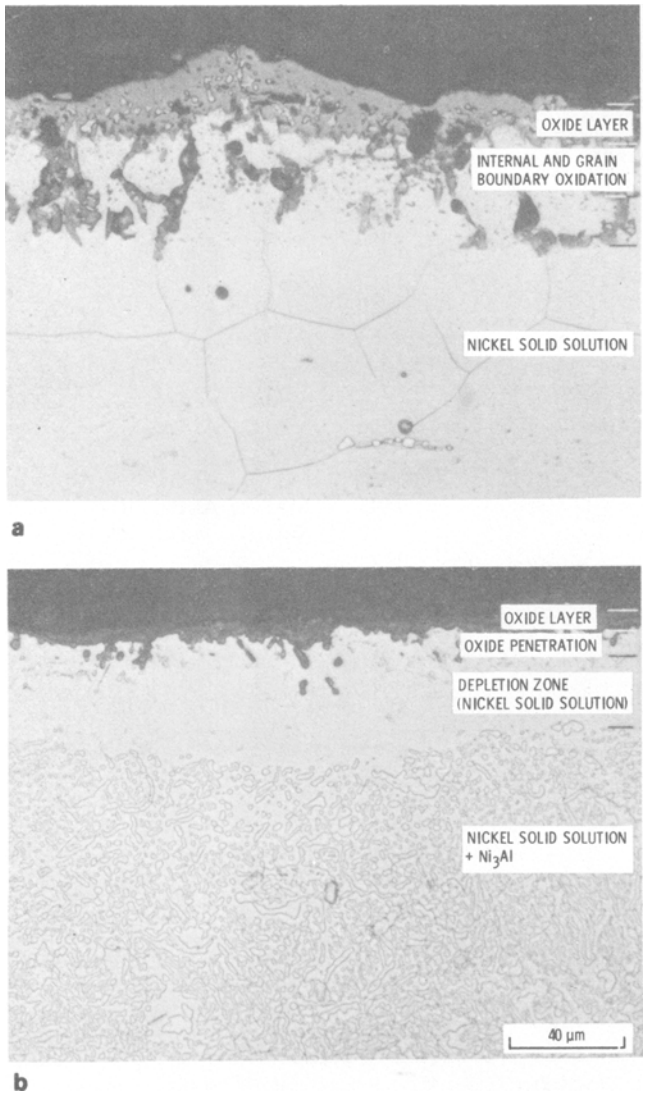

Fig. 4. Continuous oxide layers formed on IN-601 (a) and B-1900+Hf (b) after 195 cycles with $\Delta T = 1300°C$. Etched.

occurred within the oxide layer for all of the other alloys studied and not, as observed in experimental alloys by Tien and Pettit,[5] at the oxide–metal interface. The surface morphology suggests that the spalling process is certainly not uniform but occurs at seemingly random sites.

Table III. X-Ray Diffraction Results: Oxides on Surface After 195 One-Hour Cycles

Alloy	T_{max}, °C	ΔT, °C	Oxides found
HOS-875	1200	0	Al_2O_3
		1050	Al_2O_3
		1145	Al_2O_3
		1400	Al_2O_3
TD-NiCrAl	1200	0	Al_2O_3
		1050	Al_2O_3, $NiAl_2O_4$
		1145	Al_2O_3, $NiAl_2O_4$
		1400	Al_2O_3, $NiAl_2O_4$
IN-702	1200	0	$NiAl_2O_4$, Al_2O_3
		500	$NiAl_2O_4$, Al_2O_3
		800	$NiAl_2O_4$, Al_2O_3
		1050	$NiAl_2O_4$, Al_2O_3
		1145	$NiAl_2O_4$, Al_2O_3, TiO_2
		1400	$NiAl_2O_4$, Al_2O_3, TiO_2
IN-601	1100	0	Cr_2O_3
		400	Cr_2O_3
		700	Cr_2O_3, $NiCr_2O_4$, NiO
		950	Cr_2O_3, $NiCr_2O_4$, NiO
		1045	Cr_2O_3, $NiCr_2O_4$, NiO
		1300	Cr_2O_3, $NiCr_2O_4$, NiO
B-1900+Hf	1100	0	HfO_2, $NiAl_2O_4$, Al_2O_3, Tapiolite
		400	HfO_2, $NiAl_2O_4$, Al_2O_3, Tapiolite
		700	HfO_2, $NiAl_2O_4$, Al_2O_3, Tapiolite
		950	HfO_2, $NiAl_2O_4$, Al_2O_3, Tapiolite
		1045	HfO_2, $NiAl_2O_4$, Al_2O_3, Tapiolite
		1300	HfO_2, $NiAl_2O_4$, Al_2O_3, Tapiolite

Table IV. X-Ray Diffraction Results: Oxides on Surface After Various Numbers of Cycles

Alloy	T_{max}, °C	ΔT, °C	Cycles	Oxides found
718	1100	0	95	Tapiolite, Cr_2O_3
		560		Cr_2O_3, Tapiolite
		870		Cr_2O_3, Tapiolite
		930	65	Cr_2O_3, Tapiolite
		1030	45	Cr_2O_3, Tapiolite, $NiCr_2O_4$
718 coated	1100	0	360	Al_2O_3
		780	370	Al_2O_3
		1030	160	Al_2O_3

X-Ray Diffraction

The results of *in situ* x-ray diffraction of the surface of the materials after cyclic oxidation are summarized in Tables III and IV. Not shown, but found in all cases was a diffraction pattern for the underlying metal or coating. This indicates complete x-ray penetration of the oxide layer, minimizing the possibility of an undetected oxide phase.

The oxides on HOS-875 samples were found to be only alumina under all test conditions, as were those on aluminide-coated IN-718. TD-NiCrAl formed only Al_2O_3 during isothermal oxidation, but in all the other tests nickel aluminate ($NiAl_2O_4$) was also present. Similarly, IN-601 formed only Cr_2O_3 during isothermal test, but when spalling occurred ($\Delta T > 400°C$) nickel chromite ($NiCr_2O_4$) and nickel oxide (NiO) also formed. IN-702 formed Al_2O_3 and $NiAl_2O_4$ under all conditions, and when $\Delta T > 1050°C$ titanium dioxide (TiO_2) was also found.

The two cast alloys, which contain appreciable amounts of refractory metals, formed tapiolite [$Ni(Nb, Ta)_2O_6$] under all conditions. The only other oxide found in IN-718 was Cr_2O_3, except for some $NiCr_2O_4$ after $\Delta T = 1030°C$ testing. B-1900+Hf had the most complex oxide formation with hafnium dioxide (HfO_2), $NiAl_2O_4$, Al_2O_3, and tapiolite formed under all test conditions.

Specific Weight Change

The data of specific weight change ($\Delta W/A$) vs cycles at various ΔT values are plotted in Figs. 5(a)–(g). The $\Delta W/A$ for each alloy at the end of test is plotted against ΔT in Figs. 6(a) and (b).

HOS-875 [Fig. 5(a)] shows no measurable effect of ΔT. Within experimental error (~10%) the $\Delta W/A$ curves are the same for all ΔT values including isothermal. This indicates that little or no spalling of Al_2O_3 occurs in this alloy, even when cooled from 1200°C to liquid-nitrogen temperature. This was a unique alloy–oxide combination in this study. Spalling does occur in TD-NiCrAl [Fig. 5(b)]. However, a ΔT of greater than 1050°C is needed before spalling becomes obvious. As ΔT becomes larger spalling increases without any sign of leveling out even at $\Delta T = 1400°C$.

A very interesting phenomenon occurs in the spalling of IN-702. There are several distinct stages in the process once a ΔT of greater than 500°C is used. There is an initial rapid weight gain, corresponding to the isothermal test, followed by a rapid weight loss. Unpublished high-temperature diffraction data indicates that this is due to the formation and spallation of NiO. As the NiO spalls, the corresponding shift in metal composition favors the formation of Al_2O_3 and $NiAl_2O_4$. This scale composition apparently forms and spalls at a slower rate than NiO. After the rapid weight loss, the $\Delta W/A$

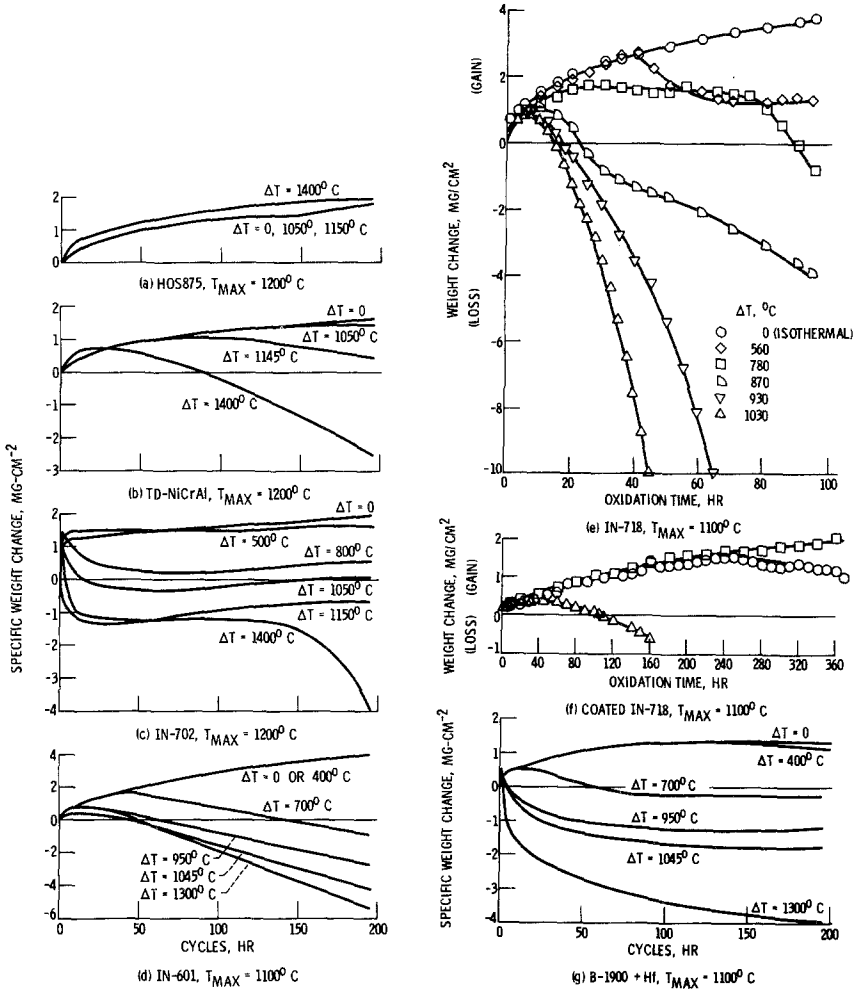

Fig. 5. Effect of ΔT on cyclic oxidation weight change.

slope became zero, and then slightly positive. If the process continues long enough (as happens at $\Delta T = 1400°C$) the metal composition can shift back, NiO forms, and the spalling rate again increases.

IN-601 [Fig. 5(d)] behaves similarly to TD-NiCrAl except that a smaller ΔT ($< 700°C$) is needed for spalling to become apparent. Similarly, bare and coated IN-718 [Figs. 5(e) and (f), respectively] have relatively simple ΔT responses. However, bare IN-718 spalls substantially with a ΔT

of only 560°C, while the coated alloy spalls only slightly at $\Delta T = 780$°C.

B-1900+Hf shows [Fig. 5(g)] a ΔT response similar to IN-702 with multistage spalling. High-temperature diffraction was also used to determine the mechanism. It proved to be similar to but slightly more complex than that for IN-702. The initial rapid gain and loss came from NiO, $NiCr_2O_4$, and Cr_2O_3. The second stage is similar to the IN-702 in that the major oxides formed are Al_2O_3 and $NiAl_2O_4$, but there are also appreciable amounts of HfO_2 and tapiolite.

In summary, at a given T_{max}, a ΔT can be found for almost every alloy below which spalling will not occur (Fig. 6 and Table V). Furthermore, no

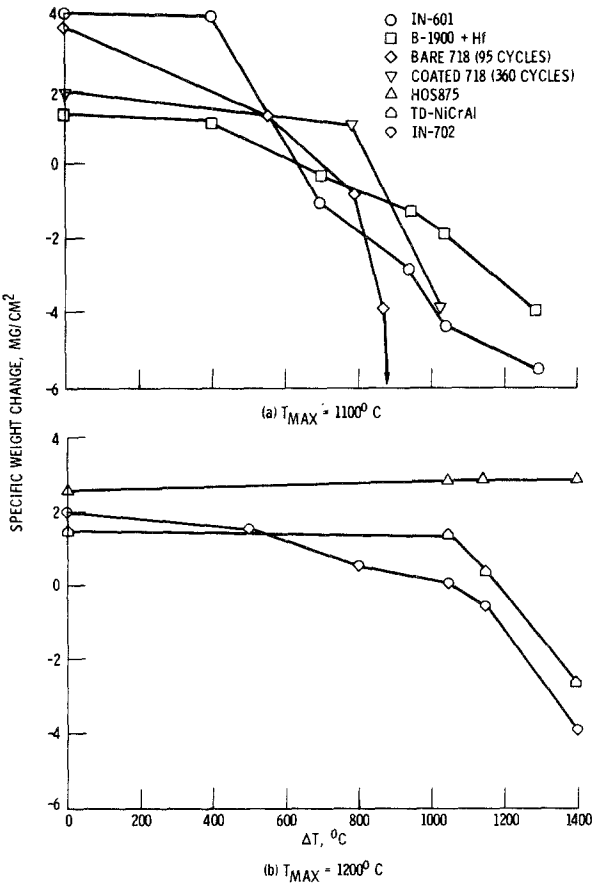

Fig. 6. Effect of cooling temperature on specific weight change after 195 one-hour cycles, except as noted.

Table V. Specific Weight Change

Alloy	T_{max}, °C	ΔT, °C	Total cycles	$\Delta W/A$, mg/cm^2
HOS-875	1200	0	195	+2.6
		1050		+2.9
		1150		+2.9
		1400		+2.9
TD-NiCrAl	1200	0	195	+1.6
		1050		+1.4
		1150		+0.4
		1400		−2.5
IN-702	1200	0	195	+2.0
		500		+1.6
		800		+0.6
		1050		+0.1
		1150		−0.6
		1400		−3.9
IN-601	1100	0	195	+4.1
		400		+4.0
		700		−1.0
		950		−2.8
		1050		−4.3
		1300		−5.5
B-1900+Hf	1100	0	195	+1.4
		400		+1.2
		700		−0.2
		950		−1.2
		1050		−1.8
		1300		−3.9
IN-718	1100	0	95	+3.8
		560		+1.4
		780		−0.7
		870		−3.8
		930	65	−9.8
		1030	45	−9.8
IN-718 coated	1100	0	360	+2.1
		780	360	+2.1
		1030	160	−0.6

ΔT was found such that increasing ΔT resulted in no more spalling even with cooling far beyond normal test conditions. The one exception to this was HOS-875, for which no evidence of spalling could be found even at $\Delta T = 1400$°C.

DISCUSSION

Evaluation of the results of this investigation leads to the conclusion that thermal expansion mismatch stresses are of major importance in the oxide spalling process. As ΔT increases, the stress in the oxide increases until the stress exceeds the strength of the oxide and failure, i.e., spalling occurs. An often quoted expression for this stress was cited by Oxx,[6] and is as follows:

$$\sigma_{ox} = \frac{E_{ox}\,\Delta T(\mathrm{CTE}_{ox} - \mathrm{CTE}_m)}{1 + 2\dfrac{E_{ox}}{E_m}\dfrac{t_{ox}}{t_m}} \tag{1}$$

where

σ_{ox} = stress in oxide, N/m^2
E_{ox} = elastic modulus of oxide, N/m^2
ΔT = difference between oxidizing temperature and temperature to which sample is cooled, °C
CTE_{ox} = coefficient of thermal expansion of oxide over ΔT, $°C^{-1}$
CTE_m = coefficient of thermal expansion of metal over ΔT, $°C^{-1}$
E_m = elastic modulus of metal, N/m^2
t_{ox} = thickness of oxide, cm
t_m = thickness of metal, cm

Since $t_{ox} \ll t_m$, the expression reduces to:

$$\sigma_{ox} = E_{ox}\,\Delta T\,\Delta\mathrm{CTE} \tag{2}$$

The foregoing neglects any growth stress contribution which, together with a lack of modulus data, makes exact stress calculation extremely difficult. However, qualitative evaluations can be made from the thermal expansion data in Table VI.[2,7,8,9,10] These are shown schematically in Fig. 7. While the details vary from alloy to alloy, in all cases the oxide is in compression while the metal is in tension. Thus failure, if it occurs by this mechanism, will be compressive. Note that the CTEs of the metallic phases are substantially the same except for the body-centered cubic alloy Hoskins-875. Its CTE is lower and would result in less compressive stress. Inserting values in Eq. (2) for $\Delta T = 1175$ and a modulus from Ref. 11 gives $\sigma_{ox} = 49 \times 10^4$ psi, which is approximately the same as the compressive strength, 45×10^4 psi.[11] This may be why HOS-875 does not spall as compared to TD-NiCrAl ($\sigma_{ox} = 67 \times 10^4$) and IN-601.

In addition to the insight gained from this investigation into the mechanisms of spalling, it has important implications for cyclic oxidation testing methods. Table VII is taken from Fig. 6 and lists the slopes of the

Table VI. Thermal Expansion Coefficients

Phase	Temperature range, °C	Mean CTE, $\times 10^{-6}$	Reference
γ-Ni solid solution	25–1200	18.6	7
γ'-Ni_3Al	25–1200	18.6	7
β-NiAl	25–1200	19.5	7
α-Fe solid solution	25–1200	15.8	Unpubl. data
TD-NiCrAl	25–1200	19.3	Unpubl. data
Al_2O_3	25–1200	8.1	8
Cr_2O_3	25–1200	8.7	9
$NiAl_2O_4$	25–1200	10	10
$NiCr_2O_4$	25–1200	10	10
NiO	25–1000	17.1	2

$\Delta W/A$ vs ΔT curves near room temperature. These data show that care must be taken to control (or determine) cooling temperatures as well as oxidizing temperatures when running cyclic oxidation tests. For example, IN-702 tested for 195 one-hour cycles at 1200°C would yield a $\Delta W/A$ of -0.85 mg/cm^2 if the cooling temperature was 25°C and -0.25 mg/cm^2 if the

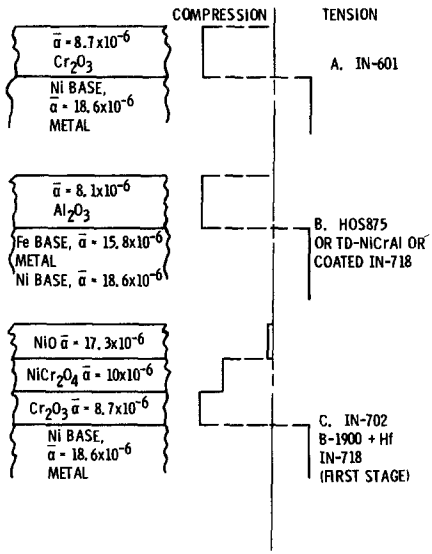

Fig. 7. Distribution of stresses after cooling from oxidizing temperature.

Table VII. Slope of $\Delta W/\Delta T$ Near Room Temperature

Alloy	Slope, $\mu g \cdot cm^{-2} \cdot °C^{-1}$	T_{max}, °C
HOS-875	0	1200
TD-NiCrAl	11	1200
IN-702	13	1200
B-1900+Hf	8	1100
IN-601	5	1100
IN-718	250	1100
IN-718 coated	7	1100

cooling temperature was 100°C—not a large difference. However, since the slopes are not the same for all materials, a variation in the cooling temperature could lead to marked changes in ranking of materials in addition to their absolute values. Therefore, when cycle oxidation test data are reported the ambient cooling temperature should be listed as well as the test temperature.

For example, in this laboratory, the standard cyclic oxidation test cools the sample from 1100–1200°C to about 66°C in 5 to 10 min before it is recycled. When it is weighed, intermittently, it cools to about 26°C. Whether this difference is significant for a given alloy within the scatter of a test remains to be determined. It is thought to be at most a second-order effect. If the sample at one laboratory were cooled to significantly higher or lower temperatures the dfferences could be major. If the samples are removed for intermittent weighing, however, the typical cooling ambient temperature should be as close to the weighing temperature as possible.

CONCLUDING REMARKS

An awareness that a primary cause of oxide spallation in cyclic oxidation testing is thermal expansion mismatch leads to attempts to alter oxide and/or metal CTEs. If the former approach is made, the direction should be toward higher coefficient of thermal expansion values; however, this must not be at the expense of greatly increased rates of formation. For example, NiO is one of the few oxides whose coefficient of thermal expansion matches that of the metal from which it forms, and indeed NiO does not usually spall from Ni. Unfortunately, the rate of oxide formation is so high that the resultant metal consumption rate is higher than that of a spalling Al_2O_3 former, e.g., TD-NiCrAl, even in a cyclic test.[12] On the other hand the metal CTE could be lowered. For example, FeCrAl is already acceptably low and perhaps other alloy systems may offer potential, as in the high-Cr alloys in the NiCrAl system as suggested in Ref. 7. All in all, however, there does not

appear to be great hope in changing CTE values with small compositional changes of either the oxide or metal, as can be seen in Table VI and Refs. 7, 8, 9, and 10.

On a more positive note, the results of this investigation do suggest ways of modeling the spalling process that should be pursued. Once developed, such a model, if accurate, would allow predictions of long-time cyclic oxidation behavior from relatively short-term testing. Such attempts have been made[12] primarily by curve fitting without trying to use a detailed understanding of the spalling process. A knowledge of the basic factors affecting oxide spalling should allow a more straightforward approach to modeling. While this investigation provides input toward dealing with part of the modeling problem, a knowledge of the effects of other variables such as cycle frequency, cooling rate, etc., will also be needed.

REFERENCES

1. C. A. Barrett and C. E. Lowell, *Oxid. Met.* **9**, 307 (1975).
2. D. L. Douglass, *Oxidation of Metals and Alloys* (American Society of Metals, Metals Park, Ohio, 1971), pp. 137–156.
3. P. Hancock and R. C. Hurst, *Advances in Corrosion Science and Technology*, M. G. Fontana and R. W. Staehle, eds. (Plenum Press, New York, 1974), Vol. 4, pp. 1–84.
4. J. R. Johnston and R. L. Ashbrook, "Effect of Cyclic Conditions on the Dynamic Oxidation of Gas Turbine Superalloys," NASA TN D-7614 (April 1974).
5. J. K. Tien and F. S. Pettit, *Metall. Trans.* **3**, 1587 (1972).
6. G. D. Oxx, *Prod. Eng. (N.Y.)* **29**, 61 (1958).
7. C. E. Lowell, R. G. Garlick, and B. Henry, "Thermal Expansion in the Nickel–Chromium–Aluminum and Cobalt–Chromium–Aluminum Systems to 1200°C," NASA TM X-3268 (August 1975).
8. P. J. Baldock, W. E. Spindler, and T. W. Baker, "An X-Ray Study of the Variation of the Lattice Parameters of Alumina, Magnesia and Thoria up to 2000°C," AERE-R5674, United Kingdom Atomic Energy Authority Research Group, Harwell (England) (January 1968).
9. O. H. Kirkorian, "Thermal Expansion of High Temperature Materials," UCRL-6132, Lawrence Radiation Lab., University of California, Livermore, Calif. (September 6, 1960).
10. I. Zaplatynsky, "Thermal Expansion of Some Nickel and Cobalt Spinels and Their Solid Solutions," NASA TN D-6174 (February 1971).
11. J. D. Latva, *Met. Prog.* **82**, 97 (1962).
12. C. A. Barrett and C. E. Lowell, "Resistance of Nickel–Chromium–Aluminum Alloys to Cyclic Oxidation at 1100° and 1200°C," NASA TN D-8255 (1976).